3.3.2.2 Photoelasticity Phase Analysis

The V-notch region is masked in all the phase and stress fields to prevent unwrapping errors and to eliminate the region in the field of view with no polycarbonate. The wrapped isoclinic angle calculated using Equation (3.3), as shown in Figure 3.9(a), contains apparent $\pi/2$ phase jumps in regions near $\sin(\delta) = 0$ throughout the field, most likely due to the nonzero tolerance of $(T_x - T_y)$ and $e_1 \neq 0$, but only a very small region on the notch edge near the notch tip actually requires unwrapping. The ambiguous wrapped isochromatic phase based on this wrapped α is shown in Figure 3.9(b), where the ambiguity appears only near the notch tip. This particular wrapped α field does not have the false zero-crossings, but only has false $\pi/2$ discontinuities where the wrapped δ is zero or $\pm\pi$.

Figure 3.9(c) is the theoretical wrapped α that incorporated beamsplitter transmission coefficients $T_x = 0.42$ and $T_x = 0.39$, which are plausible coefficients for the beamsplitter used in this study, based on manufacturer specifications and monitoring the voltage output from a photodiode collecting the transmitted (and reflected) light from the beamsplitter with pure $E_x\hat{\imath}$ or $E_y\hat{\jmath}$ input. The later method is a crude estimate of the transmission and reflectance coefficients. The modulation of the wrapped data near where the theoretical $\sin(\delta) \to 0$ is modest and does not reflect the extent of the false phase discontinuities in the experimental data except near $\theta = 0$. Figure 3.9(d) is the theoretical wrapped α including the error in the first $\lambda/4$ plate of $e_1 = \pi/90$ radians, which is small but possible given the alignment procedure of the polarization optics and the quality of the rotation mounts. This field has much greater modulation near $\sin(\delta) \to 0$, and therefore the misalignment of the first $\lambda/4$ plate is a more prominent source of error except near $\theta = 0$, where the beamsplitter T_x and T_y appear to dominate. Figures 3.9(d) and 3.9(f) are the theoretical wrapped α fields including $e_2 = -\pi/90$ radians with $e_1 = 0$ and $e_1 = \pi/90$ radians, respectively. The field including only e_2 error does not exhibit the false phase discontinuities, while the field with both e_1 and e_2 error has the false phase discontinuities and a slight shift of e_2 radians in the entire field. These theoretical fields demonstrate the types of errors that can occur, as described in Section 3.2.1, and verify that e_1 error has the greatest overall effect on the wrapped isoclinic angle.

The identified false $\pi/2$ discontinuity regions in the experimental data are eliminated and interpolated across as described in Section 3.2.4.1. The corrected wrapped isoclinic angle and the resulting ambiguous wrapped isochromatic phase are shown in Figures 3.10(a) and 3.10(b); though the ambiguous wrapped isochromatic phase does not look much different, the corrections to the wrapped isoclinic angle did smooth the δ data near $\sin(\delta) = 0$. Figures 3.10(c) and 3.10(d) show the theoretical wrapped isoclinic angle and the ambiguous isochromatic phase; the theoretical wrapped α only has phase discontinuities near the notch tip, and the only ambiguities in the wrapped δ field are near the notch tip, similar to the experimental fields. This good qualitative comparison of the experimental and theoretical wrapped data demonstrates that the correction to the wrapped isoclinic angle is acceptable. The main issue with the corrected wrapped isoclinic angle is that the corrected regions still indicate some influence from the δ data, where the wrapped α is not as radially smooth as the theoretical wrapped α. If more data points were removed and interpolated across than the $\sim 27\%$ of the data points (excluding the notch region) already corrected, then the overall nature of the isoclinic angle may have been obscured. The experimental and theoretical unwrapped isoclinic angle fields are shown in Figures 3.10(e) and 3.10(f), with good comparison except where the experimental data appear to have residual errors in the shape of the isochromatic phase that modulate the isoclinic data. For example, the experimental isoclinic angle is not as negative near $\theta = -5\pi/6$, but the regions of negative and positive α in the entire field correspond well. The theoretical isoclinic angle data in Figure 3.10(c) show a slight lobe-like structure, which is present due to the residual stresses. The isoclinic angle would only be a function of θ in a residual stress-free material, demonstrating that the theoretical solution requires inclusion of these residual stresses to compare well with the experimental data.

The experimental unambiguous wrapped isochromatic phase calculated using the unwrapped isoclinic angle, shown in Figure 3.11(a), has distinct 2π discontinuities, allowing for fast unwrapping; the resulting unwrapped isochromatic phase is given in Figure 3.11(c). The theoretical wrapped and unwrapped isochromatic phase in Figures 3.11(b) and 3.11(d) are slightly different than the experimental fields, where the wrapped data have different locations for the 2π phase discontinuities,

and the theoretical unwrapped data are smaller near the notch. These differences are expected from the theoretical images, as explained in Section 3.3.2.1. The overall shape of the isochromatic data is correct, with the double lobes slightly bent away from the y axis towards $\theta = 0$, which happens to be due to the residual stress in the material. In a residual stress-free material, the lobes of the isochromatic phase would be symmetric about the y axis.

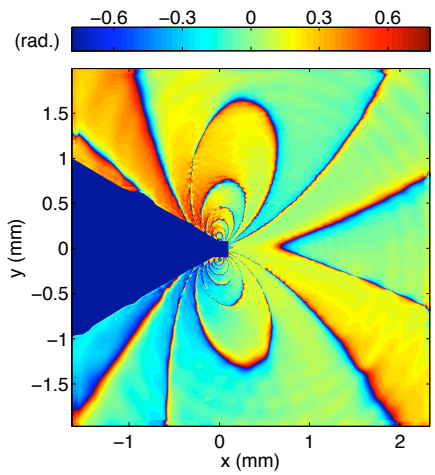

(a) Experimental wrapped α

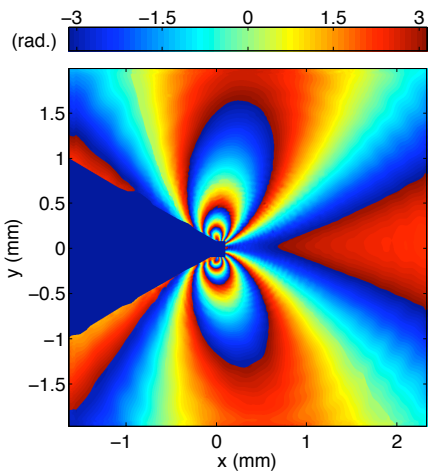

(b) Experimental ambiguous wrapped δ

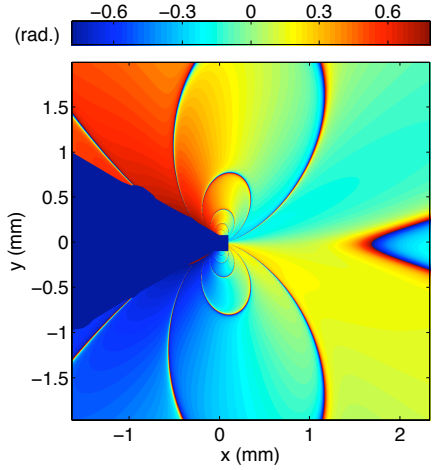

(c) Theoretical wrapped α with $T_x = 0.42$ and $T_y = 0.39$

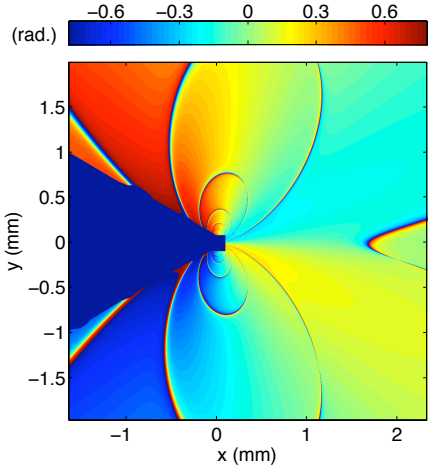

(d) Theoretical wrapped α with $e_1 = \pi/90$

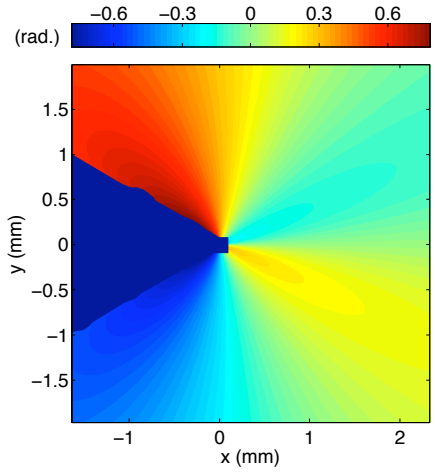

(e) Theoretical wrapped α with $e_2 = -\pi/90$

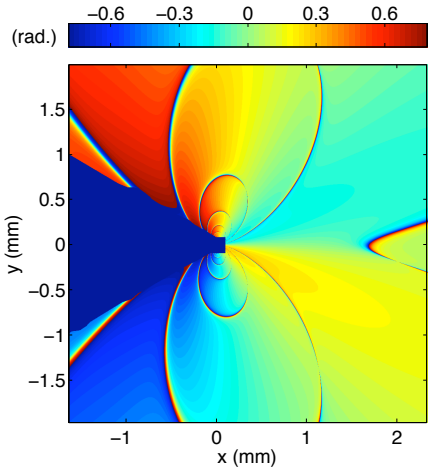

(f) Theoretical wrapped α with $e_1 = \pi/90$ and $e_2 = -\pi/90$

Figure 3.9: Photoelasticity wrapped isoclinic angle with possible error sources modeled for the compressed polycarbonate V-notch specimen with V-notch region masked in blue

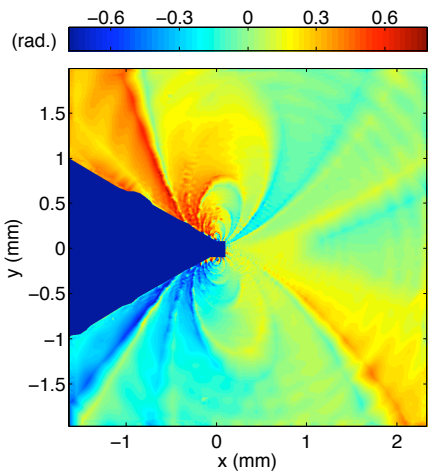

(a) Experimental corrected wrapped α

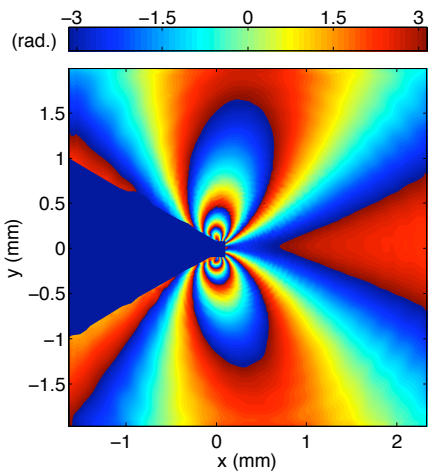

(b) Experimental ambiguous wrapped δ from corrected wrapped α

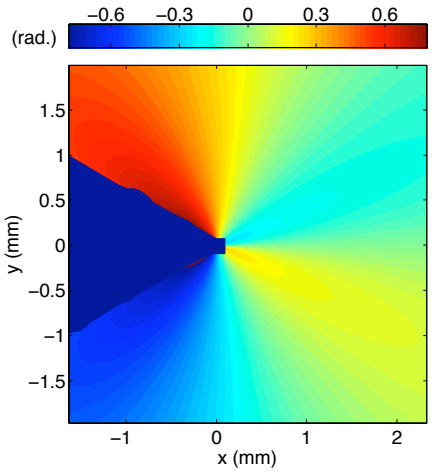

(c) Theoretical wrapped α

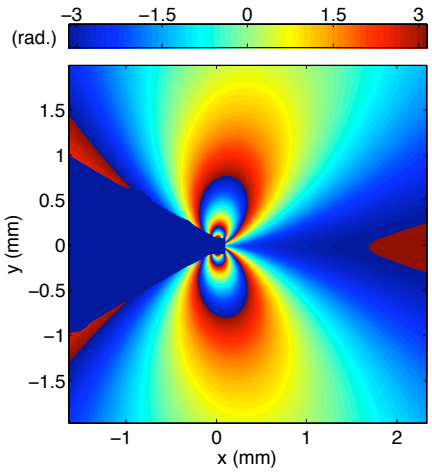

(d) Theoretical ambiguous wrapped δ from uncorrected wrapped α

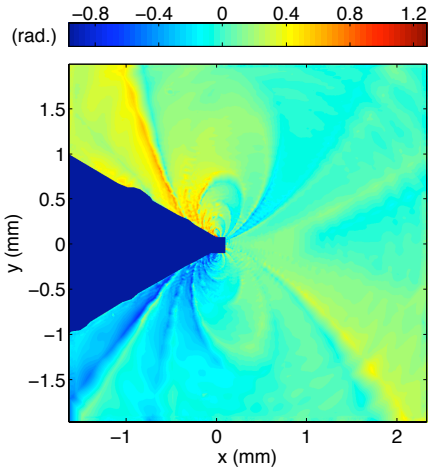

(e) Experimental unwrapped α

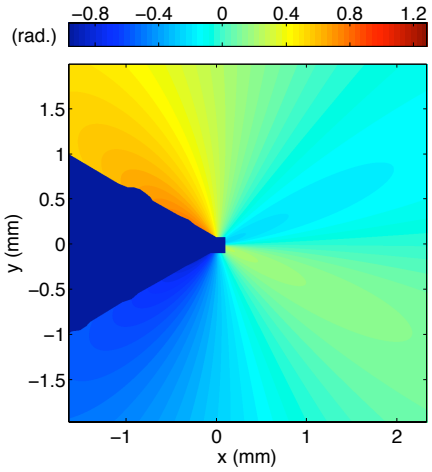

(f) Theoretical unwrapped α

Figure 3.10: Photoelasticity corrected isoclinic angle analysis for the compressed polycarbonate V-notch specimen with V-notch region masked in blue

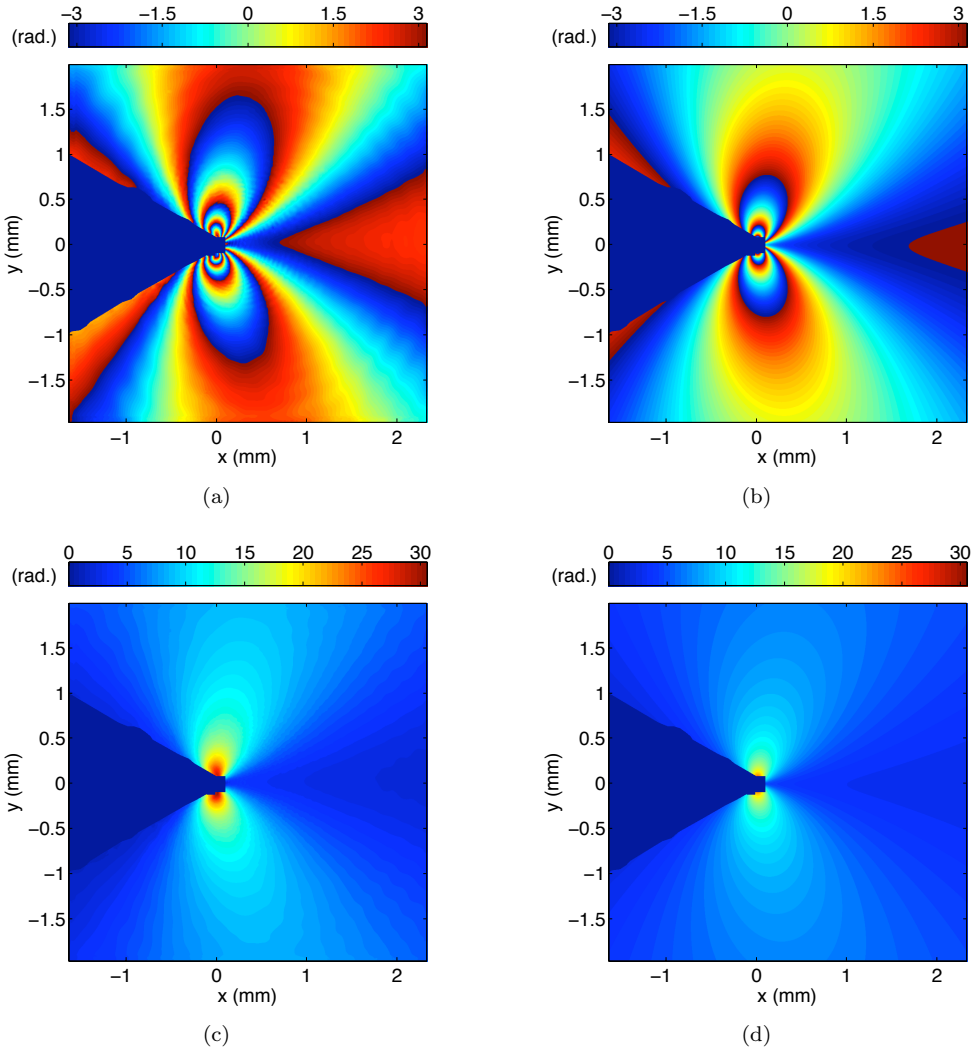

Figure 3.11: Photoelasticity isochromatic phase analysis with V-notch region masked in blue

3.3.2.3 CGS Phase Analysis

Figures 3.12 and 3.13 present the experimental and theoretical wrapped φ_{sum} for the horizontal and vertical shearing directions, respectively. The wrapped CGS phases in Figures 3.12(a) and 3.13(a) have the expected shapes and phase discontinuity density, except where poor fringe contrast in a four-lobed shape in each field disrupts the continuity of the dominant fringes. These four-lobed shapes are where $\cos(\varphi_{diff})$ is near zero in each field. Figures 3.12(c) and 3.13(c) show the theoretical $\cos(\varphi_{diff})$ fields for the horizontal and vertical shearing directions, indicating the four-lobed shapes where $\cos(\varphi_{diff})$ is near zero. These regions in the experimental data are most likely due to the $\lambda/4$ plate error e_1, which would lead to slightly elliptical polarization of the input electric field, as discussed in Section 3.2.2. These four-lobed poor fringe contrast regions are prominent in the wrapped phase quality maps, indicated by values near zero in the four-lobed shapes of $\cos(\varphi_{diff}) = 0$ in Figures 3.12(d) and 3.13(d). Due to these low-quality values in a closed shape, phase information about the monotonically increasing or decreasing phase as $r \rightarrow 0$ cannot easily pass accross the low-quality boundary. The resulting unwrapping errors appear as local phase with good quality unwrapped phase inside these four-lobed regions, but that does not have the expected either monotonically increasing or decreasing behavior as $r \rightarrow 0$. Theoretical wrapped phases assuming $e_1 = \pi/90$ radians in Figures 3.12(e) and 3.13(e), as with the photoelastic field modeling above, show the poor fringe contrast in the four-lobed shape consistent with $\cos(\varphi_{diff}) \rightarrow 0$ and exhibit similar phase modulation near these boundaries as the experimental data. Figures 3.12(f) and 3.13(f) show the theoretical poor wrapped data quality maps in the four-lobed shape for these theoretical wrapped phases including the e_1 error and show the good quality data inside the lobes away from $\cos(\varphi_{diff}) \rightarrow 0$ boundaries as in the experimental wrapped data quality maps.

The experimental unwrapped phases in Figures 3.14(a) and 3.14(c) show the types of unwrapping errors discusses above, as compared to the theoretical φ_{sum} fields that do not include e_1 error in Figures 3.14(b) and 3.14(d). The experimental data does not reach the same large phase values near the notch tip because of these unwrapping errors. Despite these local errors, the theoretical and experimental fields compare well in general shape and value away from the notch tip.

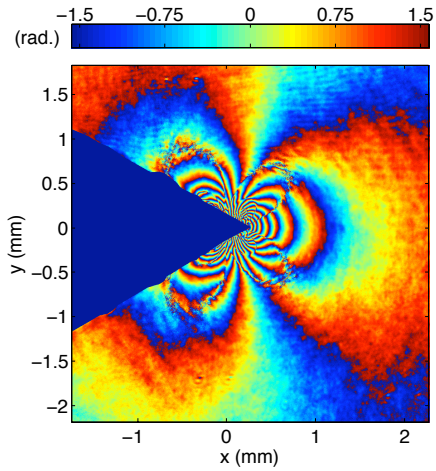

(a) Experimental wrapped φ_{sum}

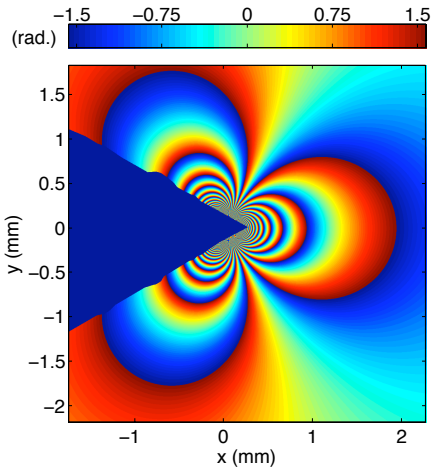

(b) Theoretical wrapped φ_{sum}

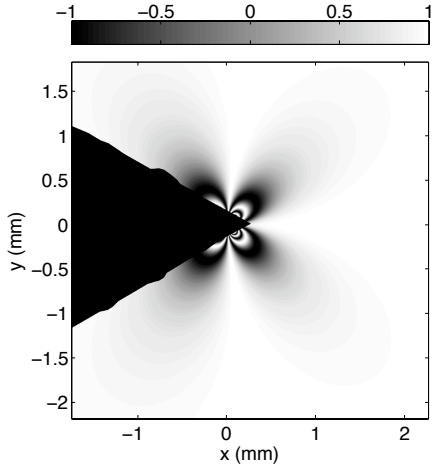

(c) Theoretical $\cos(\varphi_{diff})$

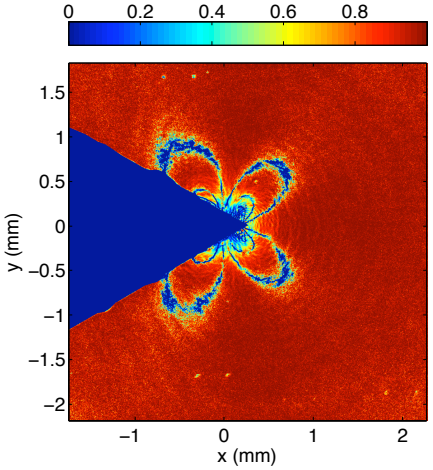

(d) Experimental phase quality map

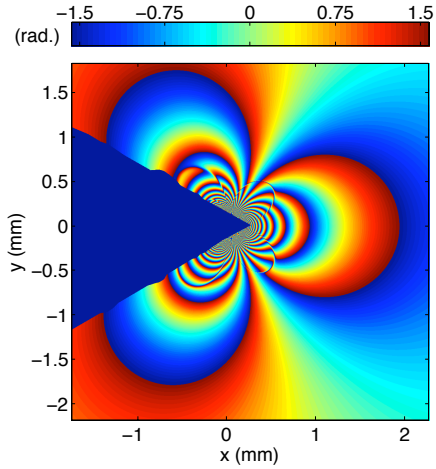

(e) Theoretical wrapped φ_{sum} with $e_1 = \pi/90$ rad.

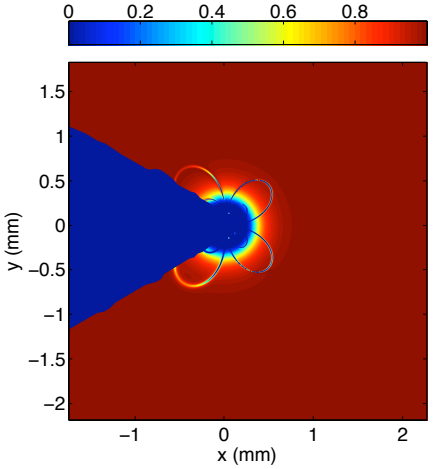

(f) Theoretical phase quality map for field with $e_1 = \pi/90$ rad.

Figure 3.12: CGS wrapped phase analysis for the horizontal shearing direction with V-notch region masked in blue (or black)

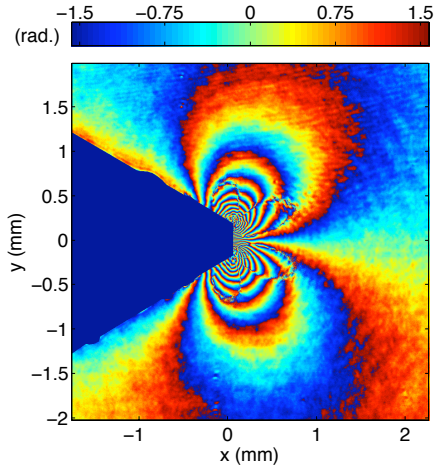

(a) Experimental wrapped φ_{sum}

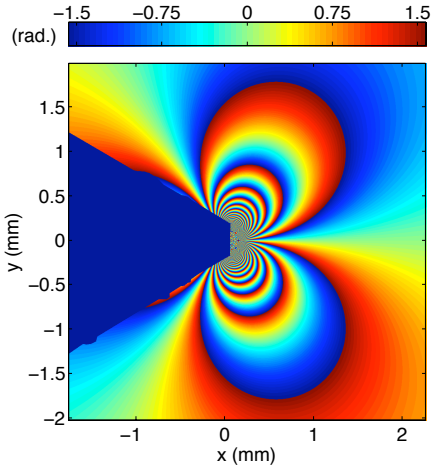

(b) Theoretical wrapped φ_{sum}

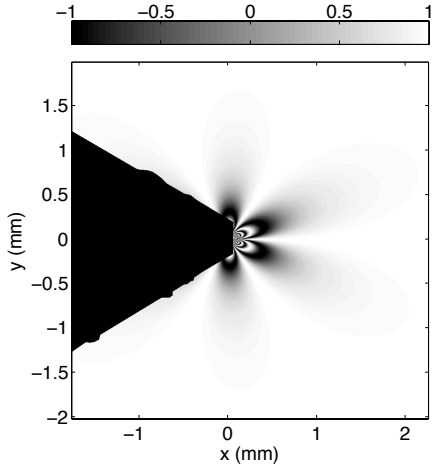

(c) Theoretical $\cos(\varphi_{diff})$

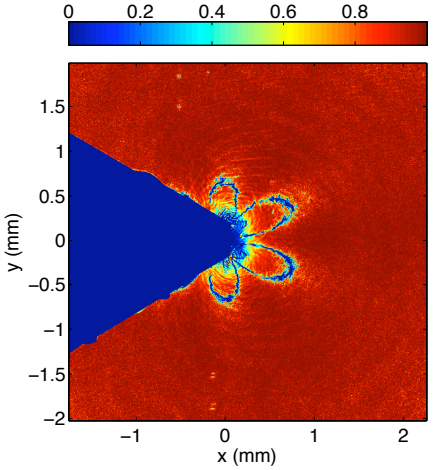

(d) Experimental Phase Quality Map

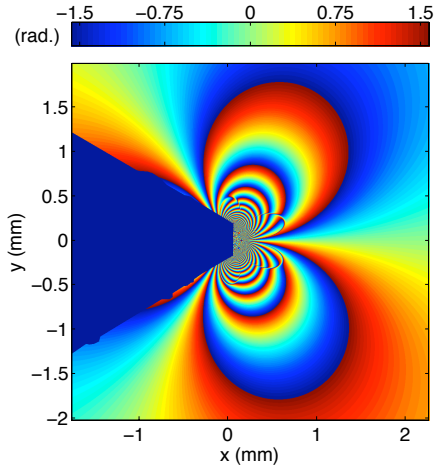

(e) Theoretical wrapped φ_{sum} with $e_1 = \pi/90$ rad.

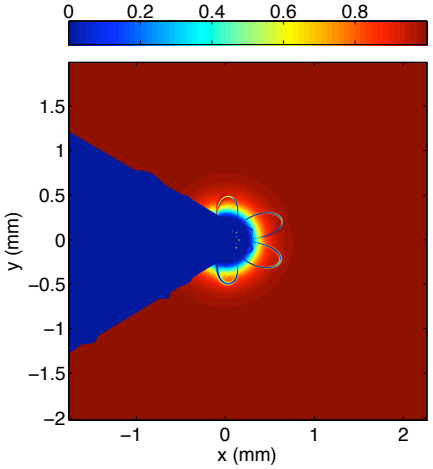

(f) Theoretical phase quality map for field with $e_1 = \pi/90$ rad.

Figure 3.13: CGS wrapped phase analysis for the vertical shearing direction with V-notch region masked in blue (or black)

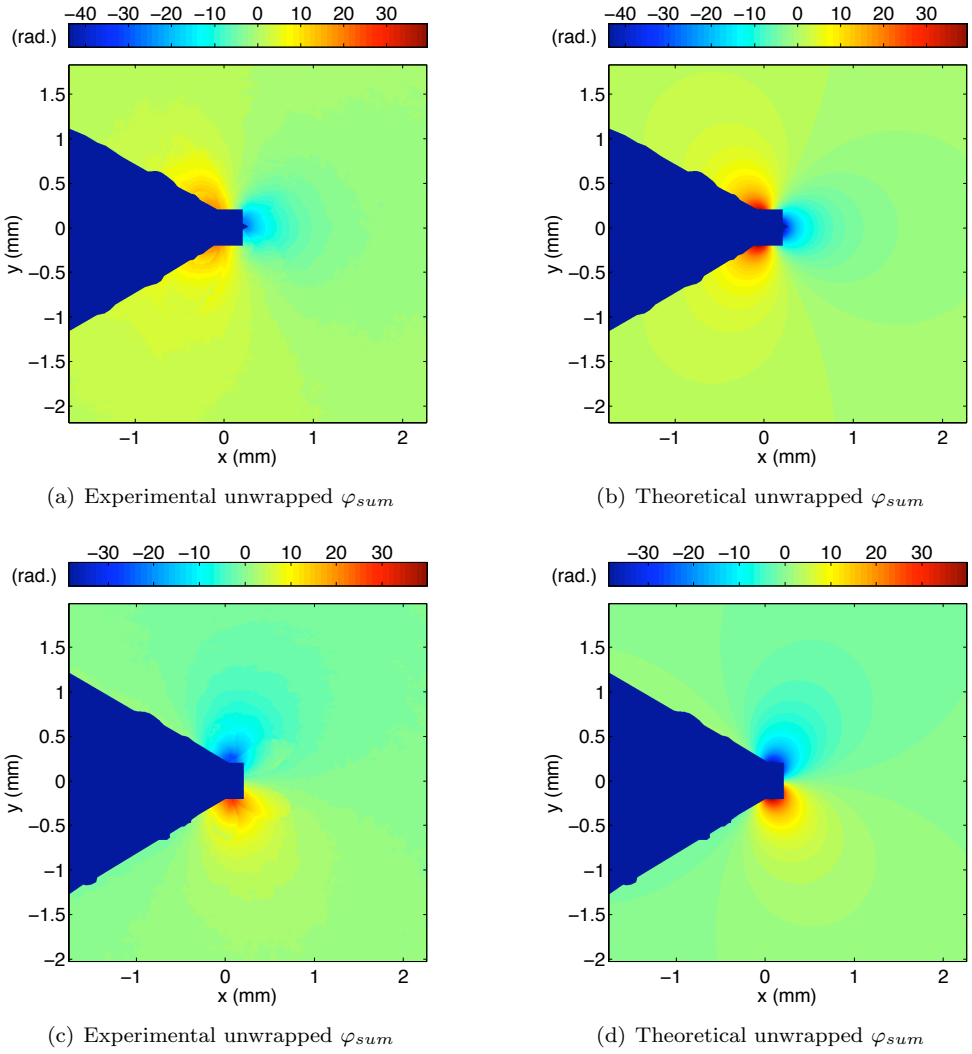

(a) Experimental unwrapped φ_{sum}

(b) Theoretical unwrapped φ_{sum}

(c) Experimental unwrapped φ_{sum}

(d) Theoretical unwrapped φ_{sum}

Figure 3.14: CGS wrapped phase analysis for the vertical shearing direction with V-notch region masked in blue (or black)